

UNCLASSIFIED

AD NUMBER	
AD037873	
CLASSIFICATION CHANGES	
TO:	unclassified
FROM:	confidential
LIMITATION CHANGES	
TO: Approved for public release; distribution is unlimited.	
FROM: Distribution authorized to U.S. Gov't. agencies and their contractors; Administrative/Operational Use; MAY 1954. Other requests shall be referred to Naval Ordnance Systems Command, Washington, DC.	
AUTHORITY	
31 may 1966, DoDD 5200.10; usnol ltr 29 aug 1974	

THIS PAGE IS UNCLASSIFIED

UNCLASSIFIED

AD NUMBER

AD037873

CLASSIFICATION CHANGES

TO:

confidential

FROM:

secret

AUTHORITY

31 may 1957, DoDD 5200.10

THIS PAGE IS UNCLASSIFIED

UNCLASSIFIED

AD _____

*Reproduced
by the*

ARMED SERVICES TECHNICAL INFORMATION AGENCY
ARLINGTON HALL STATION
ARLINGTON 12, VIRGINIA



DECLASSIFIED
DOD DIR 5200.9

UNCLASSIFIED

Armed Services Technical Information Agency

AD

37873

NOTICE: WHEN GOVERNMENT OR OTHER DRAWINGS, SPECIFICATIONS OR OTHER DATA ARE USED FOR ANY PURPOSE OTHER THAN IN CONNECTION WITH A DEFINITELY RELATED GOVERNMENT PROCUREMENT OPERATION, THE U. S. GOVERNMENT THEREBY INCURS NO RESPONSIBILITY, NOR ANY OBLIGATION WHATSOEVER; AND THE FACT THAT THE GOVERNMENT MAY HAVE FORMULATED, FURNISHED, OR IN ANY WAY SUPPLIED THE SAID DRAWINGS, SPECIFICATIONS, OR OTHER DATA IS NOT TO BE REGARDED BY IMPLICATION OR OTHERWISE AS IN ANY MANNER LICENSING THE HOLDER OR ANY OTHER PERSON OR CORPORATION, OR CONVEYING ANY RIGHTS OR PERMISSION TO MANUFACTURE, USE OR SELL ANY PATENTED INVENTION THAT MAY IN ANY WAY BE RELATED THERETO.

Reproduced by
DOCUMENT SERVICE CENTER
KNOTT BUILDING, DAYTON, 2, OHIO

ASTIA FILE COPY

THE EFFECT OF SHOCKS ON LIQUID DROPS IN THE SHOCK TUBE

4 MAY 1954



PROPERTY OF
OASD (R&D)
TECHNICAL LIBRARY

U. S. NAVAL ORDNANCE LABORATORY
WHITE OAK, MARYLAND

54AA 49485
54AA 49485

This document contains information affecting the national defense of the United States within the meaning of the Espionage Act, 50 USC, 31 and 32, as amended. Its transmission or the revelation of its contents, in any manner to an unauthorized person, is prohibited by law.

Reproduction of this matter in any form by other than naval activities is not authorized except by specific approval of the Secretary of the Navy.

NAVORD Report 3632

THE EFFECT OF SHOCKS ON LIQUID DROPS
IN THE SHOCK TUBE

Prepared by:

Robert L. Varwig

Approved by:

J. F. Moulton, Jr.
Acting Chief, Explosion Effects Division

ABSTRACT: The very small droplets produced by the fast-moving air stream when water drops are present in the shock path are about half the size assumed by G. E. Hartmann in NAVORD Report 2944, reference (3). A correction factor of one-half can be worked in by considering the effects of a transient blast suddenly applied to the drops as opposed to a gradually increasing stream velocity applied to the drops.

The smaller size droplets produced require less time to evaporate in the heated gas behind the shock front. Hence the radius of total evaporation, as discussed by Hartmann, is increased by a factor of 1.24 and the shock pressure attenuation is increased by a small amount. The numerical results of these experiments are applied to the Hartmann theory of pressure attenuation associated with an explosion in fog or rain for purposes of comparison.

Explosives Research Department
U.S. NAVAL ORDNANCE LABORATORY
White Oak, Maryland

544A

49485

~~544A 49485~~


SECRET

NAVORD Report 3632

4 May 1954

This report describes the initial work done in the Naval Ordnance Laboratory as an experimental check on some of the assumptions made in NAVORD Report 2044. This work has been carried on under Task W2c-67-1-54 by the Shock Phenomena and Shock Photography Section of the Explosion Effects Division.

EDWARD I. WOODYARD
Captain, USN
Commander


PAUL M. FYE
By direction

ii
SECRET

SECRET
NAVORD Report 3632

CONTENTS

	Page
I Introduction	1
II Method	3
III Description of the Apparatus	4
IV Results	10
V Conclusions	17

ILLUSTRATIONS

Table I	Test Results for Two Mean Peak Shock Overpressures . .	15
Table II	Values for τ in milliseconds	18
Table III	Radius of Total Evaporation, R_1 , and other Quantities for Rain	19
Table IV	Radius of Total Evaporation, R_1 , and other Quantities for Fog	20
Table V	Calculation of P_T for 1 lb of Pentolite	23
Table VI	Calculation of P_T for 20 KT Atomic Bomb	24
Table VII	Calculation of P_T for 1 megaton of Pentolite	25

Fig. 1	4 Shot Pulse Generator	5
Fig. 2	Thyratron Switching Circuit	6
Fig. 3	Shadowgraph with Four Exposures at Time Separations of 40 msec	8
Fig. 4	Shadowgraph System	9
Fig. 5	Direct Photography System	9
Fig. 6	Break-up of Drop at 2.69 psi (Direct Photography) . .	11
Fig. 7	Break-up of Drop at 2.63 psi (Direct Photography) . .	11
Fig. 8	Break-up of Drop at 1.46 psi (Shadowgraph)	12
Fig. 9	Break-up of Drop at 1.70 psi (Shadowgraph)	12
Fig. 10	Break-up of Drop at 1.90 psi (Shadowgraph)	13
Fig. 11	Size Distribution of Droplets	16
Fig. 12	Cube Root of Charge Weight $W^{1/3}$ as a Function of Radius of Complete Evaporation R_1	21

THE EFFECT OF SHOCKS ON LIQUID DROPS
IN THE SHOCK TUBE

I INTRODUCTION

1. In the detonation of explosives, there is definite experimental evidence that a loss of performance occurs when the charges are exploded in rain or fog (1). There is a percentage loss in positive blast impulse and also in peak overpressure, according to theory, which is practically linearly proportional to the concentration of liquid water in the air, provided the raindrops are of uniform size and the percentage decrease in blast performance is not great.
2. This peak pressure or shock wave attenuation has been attributed to increased energy losses resulting from the evaporation of the water droplets in the fast-moving air stream behind the shock. W. G. Penney (2) and G. K. Hartmann (3) have worked out relations leading to analytical statements regarding the loss of performance due to the presence of fog or rain.
3. The evaporation of the droplet takes place in the fast moving, heated air stream behind the shock front. The time t for the droplet to reach 99 per cent of the particle velocity and the lag L of the droplet behind the air particles are computed to be, respectively (3)

$$t = 35/P_g^{1/4} \text{ sec}$$

$$L = 8 u_g/P_g^{1/4} \text{ cm,} \quad u_g = \text{flow speed.}$$

4. The contribution to the evaporation process when the droplet is ventilated, i. e., when the air surrounding the droplet is continuously being swept away and replaced by fresh air not previously in contact with the droplet, has been considered and was found negligible.
5. After the droplet reaches the flow speed the problem is one of calculating the evaporation rate of spherical droplets in still, warm or hot air. The temperature differential, $\theta = \theta_s$, of the droplet surface and the shock temperature is shown to be $0.86 \theta_s$ where $\theta_s + T_0$ is the temperature of the air immediately behind the shock, $\theta + T_0$ is the temperature at the drop surface after the arrival of the shock and T_0 is the ambient temperature. Using the heat transfer equation, $\frac{d\theta}{dt} = K \sqrt{V} T$,

SECRET
HAYGORD Report 3632

where K is the diffusivity, the time for evaporation is calculated. It has been shown (3) that evaporation will be complete within a time τ equal to the positive duration of a blast wave if

$$\tau = 1.41 \frac{L^* A^2}{\sigma \phi_s} \text{ sec.}$$

where L^* = latent heat of evaporation = 580 cal/gm

σ = specific thermal conductivity of air

A = radius of water droplet

ϕ_s = temperature rise associated with the peak overpressure rise P_s in the shock wave.

This equation reduces to

$$\tau = \frac{3.53 A^2}{P_s} \left(\frac{P_s + 95}{90} \right) \left(\frac{62}{P_s + 67} \right)^{3/2} 10^9 \text{ msec}$$

for $P_s < 30$ psi.

6. It is necessary that the drop be stable in the fast-moving air stream while it is evaporating. A drop of water in fast-moving air is subject to aerodynamic forces due to the motion of the air, and also forces due to the surface tension in the drop itself. There is a critical drop size above which the drop is not stable for each set of forces to which it is subjected. If a drop is suddenly placed in a fast-moving air stream of velocity u , then the critical radius, a , will depend on the produce of ρ , the density of the air, and u^2 and on the surface tension. The product ρu^2 is proportional to the aerodynamic forces, i.e.

$$a \sim T_e (\rho u^2)^{-1} \quad T_e = \text{surface tension.}$$

Since the surface tension is essentially constant for the range of interest here, the critical radius varies inversely as $(\rho u^2)^{-1}$. From observation of falling water drops, when $u = 800$ cm/sec and $\rho = \rho_0$, then $a = 0.33$ cm (3), therefore:

$$a = 0.33 \frac{\rho_0}{\rho} \left(\frac{800}{u} \right)^2 \text{ cm.}$$

7. Calculating ρ and u from the Rankine-Hugoniot relations in terms of P_s , the peak shock overpressure, a relation is shown to exist between P_s and a which can be stated as:

SECRET
NAVOED Report 3632

$$P_s^2 a = 8.4 \times 10^{-2} \text{ within 5 per cent.}$$

(P_s is in psi, a is in cm.)

8. What this means then is that when a shock hits a rain drop, if the drop is greater than the critical size, it will be reduced to smaller droplets which are stable in the air stream behind the shock. For example, if a drop of radius 0.5 cm is struck by a 2 psi shock front, it will be shattered into many droplets of radius given by

$$a = \frac{8.4 \times 10^{-2}}{P_s^2} = 0.021 \text{ cm.}$$

Hartmann (3) used the above expression for the radius of the water droplets that would be totally evaporated by a shock wave of peak overpressure P_s . Further calculations were made to determine the radius of complete evaporation, R_1 (ft), as a function of charge weight, W (lbs TNT) which led to the expression

$$R_1 = 5.1 (W^{1/3})^{1.11} \text{ ft.}$$

The total energy in the shock wave at a distance $R < R_1$ was then shown to be

$$F(R) = 4.06 \times 10^5 \frac{W^{11/9}}{R^{2/3}} - 69 cR^3$$

where c = concentration of water in gm/m³.

The second term in this expression represents the loss in energy due to rain or fog.

9. The purpose of the present study was to measure the size of the droplets produced in a shock tube when a step-type shock wave hits liquid water drops introduced into the tube. In this way it is possible to ascertain the validity of the relation between shock overpressure and droplet radius upon which the expression for the radius of complete evaporation rests.

II METHOD

10. It was decided to attack the problem by taking photographs of the drop during the passage of the shock front. A high-speed, repeating

SECRET
NAVORD Report 3632

spark source was used to produce shadowgraphs after several known time intervals during which the drop and the shock interacted. This series of exposures, all recorded on the same sheet of film, depicted the behavior of the drop during the passage of the shock front and showed the subsequent break-up of the drop into droplets in the fast-moving air stream behind the shock.

III DESCRIPTION OF THE APPARATUS

11. In conducting this series of experiments, water drops were introduced into the shock tube by means of a hypodermic syringe inserted through the top of the shock tube so that only about 8 mm of the needle protruded into the tube. The syringe was cushioned in a heavy rubber stopper which was mounted flush with the interior surface of the shock tube. Thus only the needle tip was in a position to disturb the shock front.

12. The size of the water drops introduced into the shock tube was controlled by the size of the hypodermic needle. For a number 20 needle, ground off squarely at the end, the drop size was 0.25 ± 0.05 cm.

13. To get multiple shadowgraphs of the break-up of the liquid drop it was necessary to build a multiple flash unit in which a series of flashes occurred, all emanating from the same point. Since the light source was to be a spark in air, it was necessary to build a unit in which several condensers could be discharged through the same gap successively. The problem, therefore, was reduced to that of developing a switching arrangement which could switch each condenser in turn across the single gap. This was accomplished by using the circuit recommended by Benjamin Crapo, Hyperballistics Division of the Naval Ordnance Laboratory (NOL), and is shown in Figs. 1 and 2. Hydrogen thyatron tubes, type 5C22, were employed for the switches, each triggered by a pulse from the pulse generator unit. Operation was simple. The initiating pulse from the shock velocity measuring device associated with the shock tube was applied to the grid of the first 2D21 thyatron tube. The tube conducts the cathode rising. The voltage pulse from the cathode is coupled to the control grid of the 0A5; it conducts and its cathode rises. This voltage pulse in turn initiates the firing of the 5C22 thyatron, which essentially shorts the capacitor C in the plate circuit. Current surging through the inductance L causes a large voltage across the terminals of L and, therefore, across the gap. The gap breaks down discharging the capacitor through it, producing an actinic spark.

14. The cathode of the first 2D21 is connected to the control grid of the second 2D21 through delay units that were variable from one to thirty msec. Hence, the second 2D21 would conduct after a pre-determined time interval and the same train of events would occur as before, culminating in the discharge of the second



SECRET
NAVORD REPORT 3632

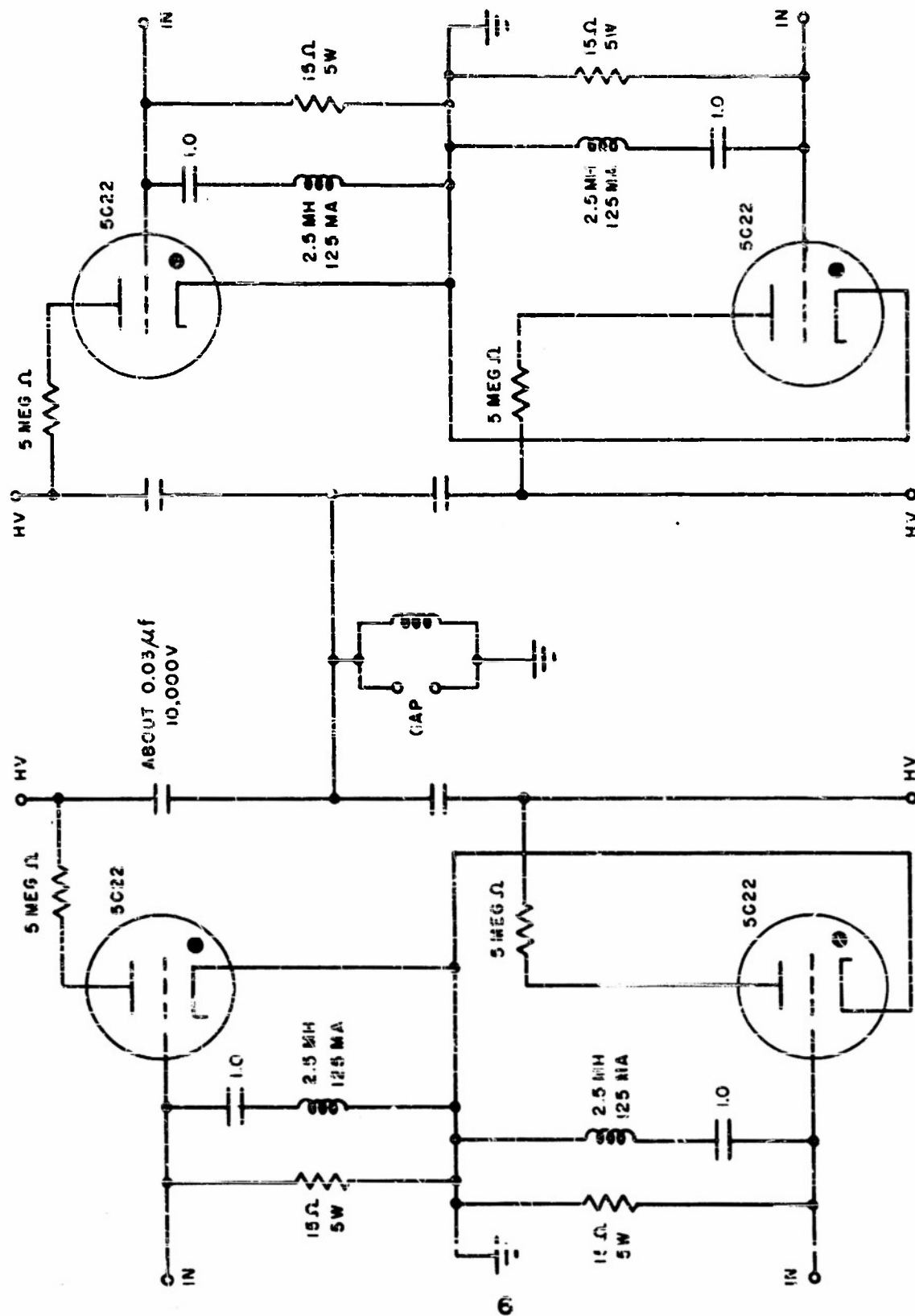


FIG. 2 SPARK UNIT

SECRET

SECRET
NAVORD Report 3632

condenser c across the gap. In this way it was possible to get four separate flashes from the spark gap at pre-determined intervals. Of course this method could be carried further to produce any desired number of spark flashes but four were sufficient in this instance.

15. The grids on the 5C22 thyratrons were required to have very low input impedances to prevent spurious discharges. Therefore, it was necessary to use a second stage of amplification in the form of the 0A5 trigger tubes to initiate conduction in the 5C22 thyratrons.

16. Originally, time intervals of $30 \mu\text{sec}$ were thought to be appropriate for photographing the drop disintegration as it was expected that the shock front produced the shattering of the drop. For this delay, ordinary LC delay lines were used with considerable success. The shadowgraphs obtained (Fig. 3), however, indicated that this time interval was too short for anything to have happened to the liquid drop. From high speed motion pictures taken with an Eastman High Speed (3000 fps) camera, it was determined that several milliseconds were required between exposures, and a time interval of up to 30 msec was introduced by employing the dual time delay unit recently developed at the NOL for other purposes (4).

17. The shadow photographic system was set up as indicated in Fig. 4. The lens 1 had a focal length of 345 mm and a relative aperture of $f/1.5$. Parallel light through the shock tube in the region under investigation produced a shadowgraph of magnification = 1. Multiple exposures were obtained on the same fixed sheet of film.

18. The shadowgraph system was eventually discarded; the arrangement shown in Fig. 5 was employed. The camera used was a 4x5 graphic view camera. The advantage of this system, using reflected light, was the greatly improved definition of the droplets after break-up. However, the shock was no longer visible in these pictures because the optical system was now not sensitive to very small density changes.

19. The droplets in the two types of photographs were measured in two ways. The droplets in the shadowgraphs were measured using a 5 x 5x magnifying eye piece which contained a millimeter scale graduated in tenths for comparison. The contrast was low and the definition of the droplets was poor so that use of a microscope with a small field and high magnifying power was prohibited. Even with the 5 power magnifier, the fuzziness of the droplets caused an uncertainty in the diameter measurements of each droplet of approximately 10 per cent. The droplets in the pictures photographed by reflected light were much more clearly defined and it was thus possible to make measurements on these droplets using a traveling microscope. The least count on the barrel of the microscope was 0.01 mm and the vernier

SECRET
NAVORD REPORT 3632

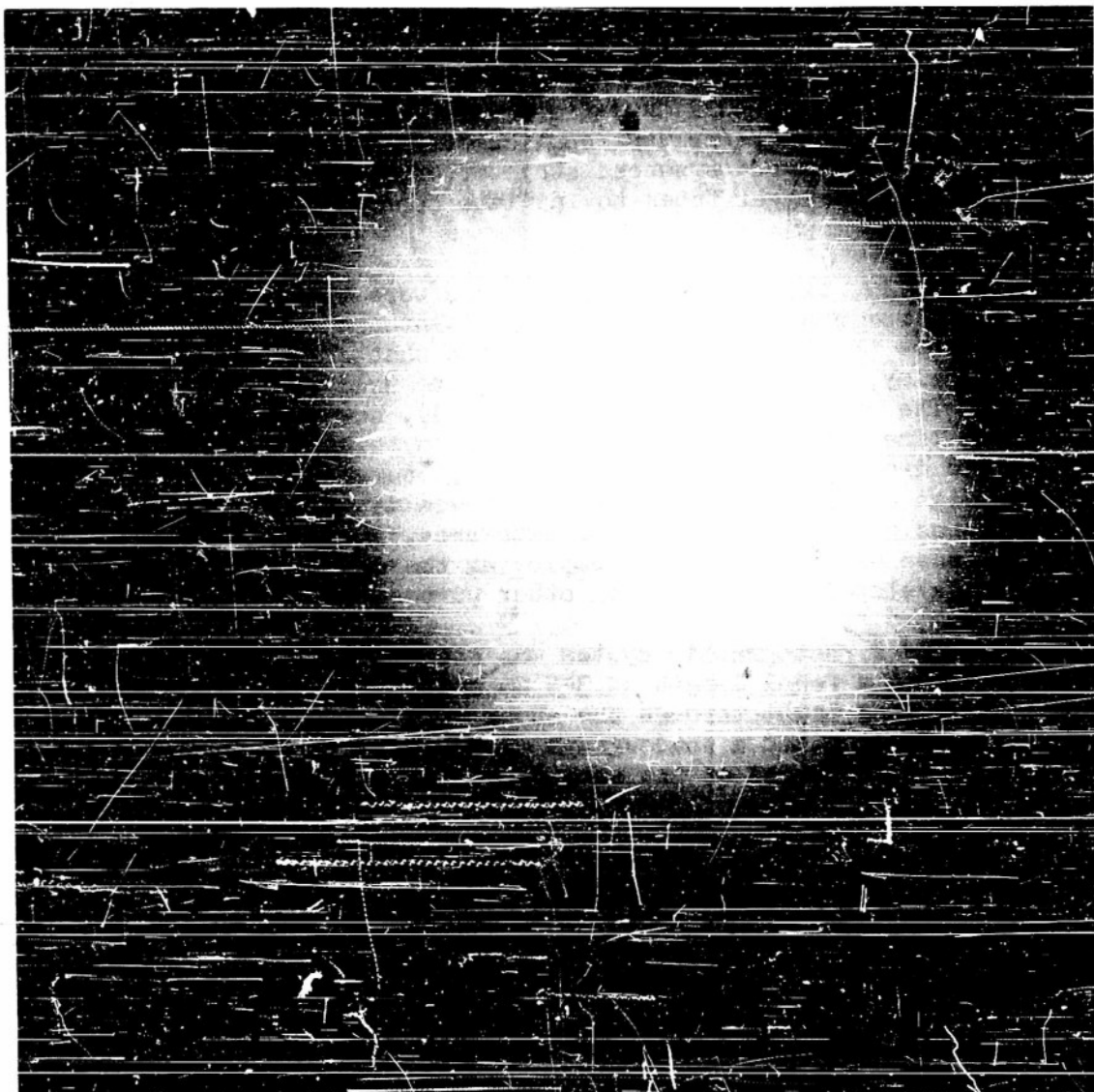


FIG. 3 TIME INTERVAL BETWEEN EXPOSURES: 40μ SEC.
SHADOWGRAPH WITH FOUR EXPOSURES

SECRET
NAVORD REPORT 3632

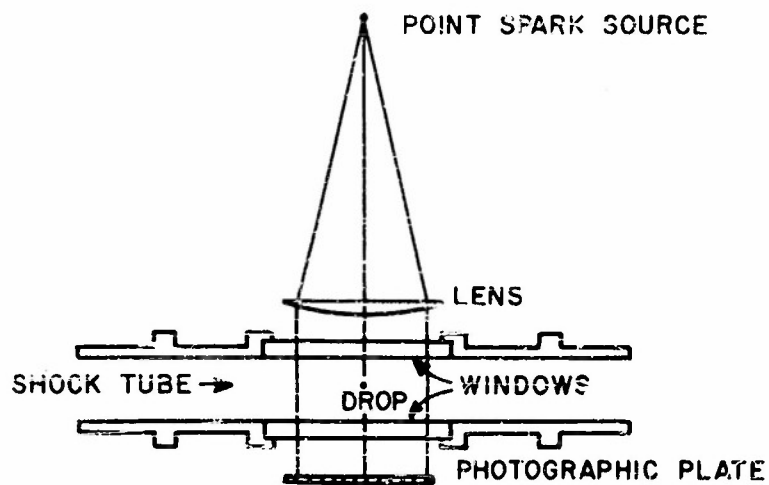


FIG. 4 SHADOWGRAPH SYSTEM. PATH OF DROP IS PERPENDICULAR TO PLANE OF PAPER.

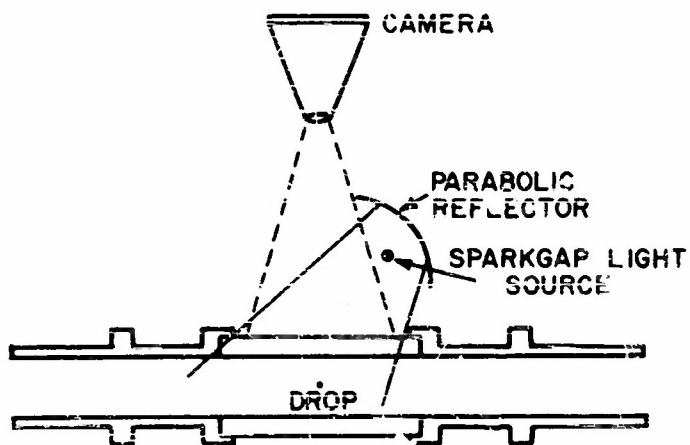


FIG. 5 DIRECT PHOTOGRAPHY SYSTEM

SECRET
NAVORD Report 3632

made possible measurements as fine as 0.001 mm. The definition of the droplets, however, was not good enough for this last figure and the uncertainty in the measurements of these records was of the order of 5 per cent.

IV RESULTS

20. The results of this study indicate the relationship between the droplet size and the shock strength, and also yield qualitative information regarding the nature of the break-up of the liquid drops.

21. The phenomenon of the shock-drop interaction is the same in nature as the sudden introduction of a drop into a fast-moving air stream. Studies of this type have been made before (5) and the apparent behavior of the drop in the shock tube is almost identical. When the drop is injected into the fast-moving air stream, the original spherical drop is distorted into a saucer-shaped disk. The edges are drawn out into streams and then they break away into droplets. (See Figs. 6, 7, 8, and 9.) At shock overpressures in the neighborhood of 2 psi, the deformation of the drop begins after about 0.8 milliseconds. However, droplets do not begin to appear earlier than about 3 milliseconds. From theoretical considerations regarding the pressure over the surface of the drop, Taylor has concluded that the drop, if it did not disintegrate, would be flattened into a plano-convex lenticular body of diameter twice that of the original spherical drop (6). In the photographs taken early enough to catch the disk-shape of the drops, this ratio seems to be confirmed by this study (see Fig. 10).

22. The size of a stable drop in a fast-moving air stream is given by the relation in the introduction of this report, i.e.,

$$a = 0.33 \left(\frac{\rho_0}{\rho} \right) \left(\frac{800}{u} \right)^2 \text{ cm.}$$

In this case the drop is in an air stream the velocity of which is gradually increased up to the critical value of u where the drop is just stable. In a transient blast of the sort used in the present study, the relation should be altered as follows:

$$a = 0.33 \left(\frac{\rho_0}{\rho} \right) \left(\frac{800}{\sqrt{2} u} \right)^2$$

SECRET
NAVORD REPORT 3632



FIG. 6 $P_s = 2.69$ PSI



FIG. 7 $P_s = 2.63$ PSI
BREAKUP OF DROP (DIRECT PHOTOGRAPHY)

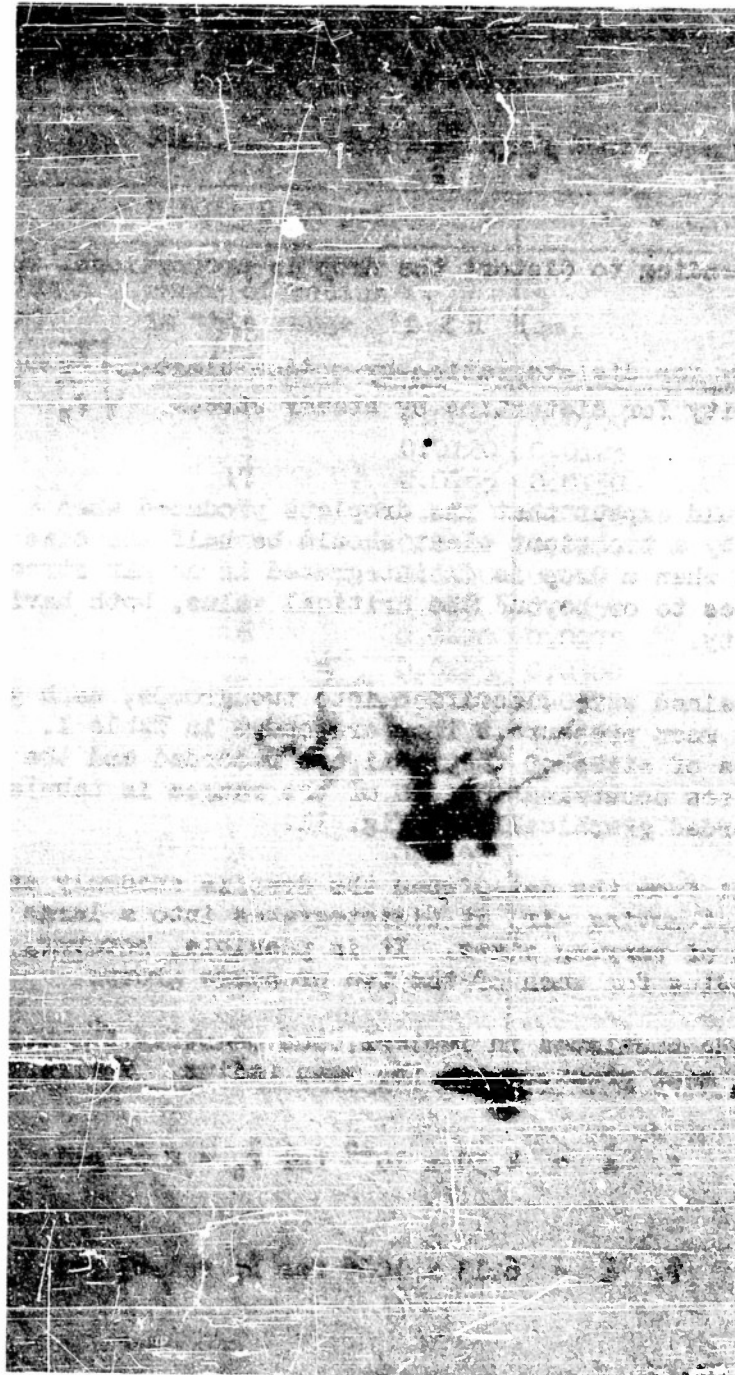
SECRET



FIG. 8 $P_s = 1.46$ PSI
BREAKUP OF DROP (SHADOWGRAPH)



FIG. 9 $P_s = 1.70$ PSI
BREAKUP OF DROP (SHADOWGRAPH)



NOTE LENTICULAR SHAPE OF ORIGINAL SPHERICAL DROP IN SECOND FLASH
AND STREAMING OUT IN THIRD FLASH. DROPLETS HAVE NOT FORMED

FIG. 10 $P_g = 1.90$ PSI

BREAKUP OF DROP (SHADOWGRAPH)

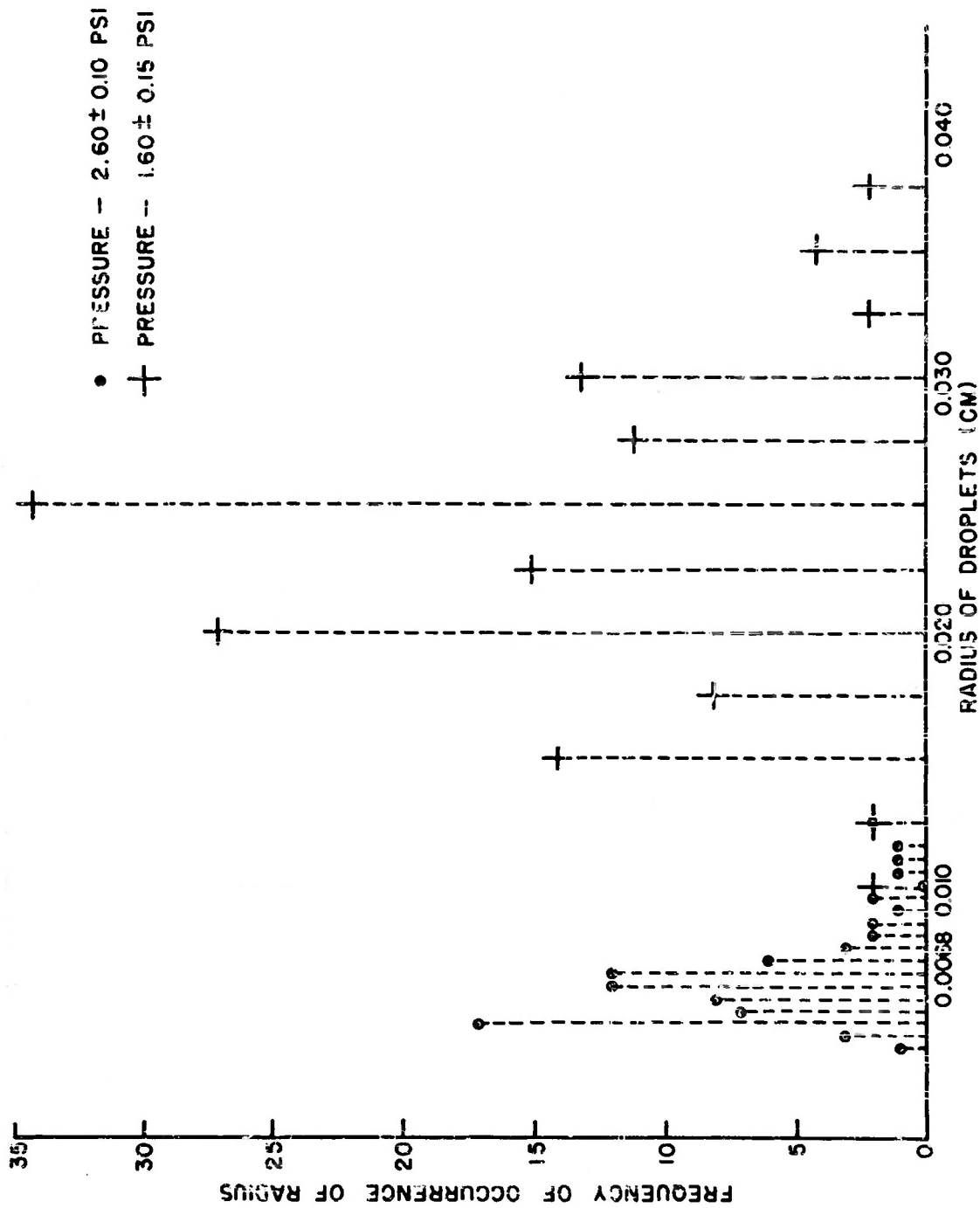


FIG. 11 SIZE DISTRIBUTION OF DROPLETS

is seen to be good agreement for the data in the range 2.60 ± 0.10 psi. In the range 1.63 ± 0.15 psi, there is a discrepancy of 30 per cent. The only explanation for this discrepancy at the present time is a negative one. The measurements on the radii for this group of data are quite unreliable since these measurements were made from shadowgraphs in which the droplets were not satisfactorily defined. It was for this reason that the photographic technique was changed as explained in section III.

V CONCLUSIONS

27. The droplets produced by the fast-moving air stream behind the shock are about half the size predicted on the basis of the report by G. E. Hartmann (3). A correction factor of 2 can be worked in by considering the effects of a transient air blast suddenly applied as opposed to a steady stream gradually applied.

28. As stated by Hartmann (3) if the drops shatter into fragments finer than those predicted on the basis of the drag forces, then the evaporation time for a droplet will be reduced by the square of the factor by which the drop is reduced. In Table II are tabulated values for the evaporation time τ in milliseconds for various drop sizes at increasing pressures. The dotted line separates the drops which break up in the fast air stream from those which are small enough to be stable in the fast air stream associated with each of the specified shock overpressures.

29. In Tables III and IV, values for R_1 , the radius of complete evaporation, and the cube root of the charge weight, $W^{1/3}$, are tabulated for rain and fog respectively. Rain is defined arbitrarily to be water drops larger in radius than 10^{-3} cm. Fog particles are defined to be $\sim 10^{-3}$ cm in radius. The values for R_1 and $W^{1/3}$ were determined as follows: The values of τ and P_2 were taken from Table II. From the Kirkwood-Brinkley curve (3) of peak overpressures versus reduced distance λ , values of λ were secured. From the graph of reduced positive phase, $\tau/W^{1/3}$, as a function of λ values of $\tau/W^{1/3}$ were obtained. $W^{1/3}$ was then calculated from knowledge of both τ , the evaporation time, and $\tau/W^{1/3}$, the reduced positive phase. Finally, $R_1 = \lambda W^{1/3}$ was computed. The graph in Fig. 12 of $W^{1/3}$ versus R_1 was plotted from these tables. The graph can be represented analytically by

$$R_1 = 6.2 (W^{1/3})^{1.11}$$

as opposed to the previous value (3) of

$$R_1 = 5.1 (W^{1/3})^{1.11}$$

The values of fog and rain agree out to the distance where evaporation occurs without break-up.

30. The expression for the energy available at a distance $R < R_1$ viz:

SECRET
NAVORD Report 3632

TABLE II

Values for τ in milliseconds

P_s	$a_0 = 1$	10^{-1}	10^{-2}	10^{-3}	10^{-4}
0.29	56.6×10^8	1.14×10^8	1.14×10^6	1.14×10^4	114
1	1.14×10^7	1.14×10^7	3.3×10^5	3.3×10^3	33
3	4.6×10^4	4.6×10^4	4.6×10^4	1.1×10^3	11
5	3.48×10^3	3.48×10^3	3.48×10^3	660	6.6
7	0.635×10^3	0.635×10^3	0.635×10^3	0.635×10^3	4.7
9	190	380	380	380	3.2
15	12.4	12.4	12.4	12.4	2.2
20	2.75	2.75	2.75	2.75	1.65
30	0.32	0.32	0.32	0.32	0.32

TABLE III

Radius of Total Evaporation, R_1 , and other
Quantities for Rain

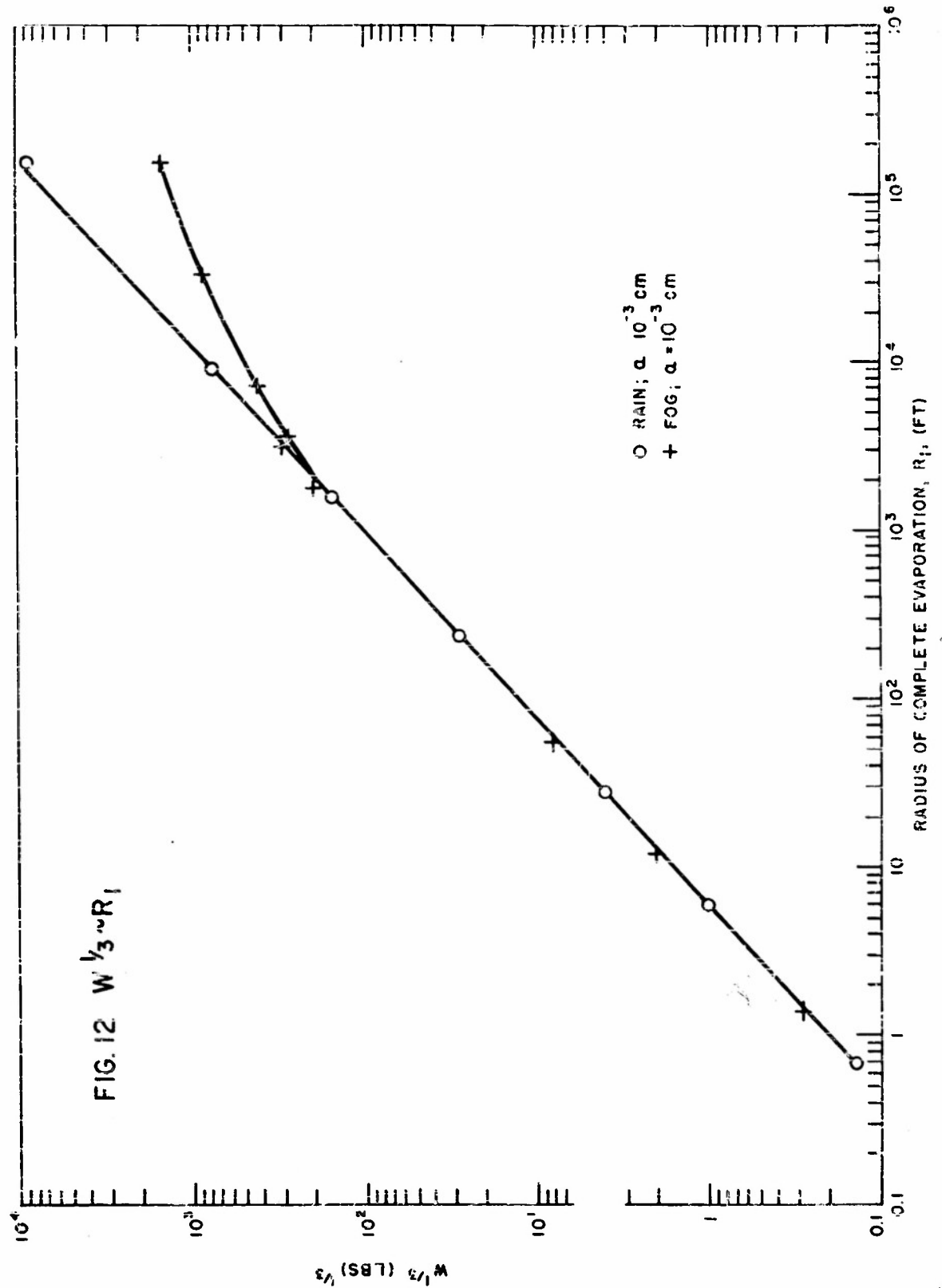
P_a (psi)	T nsec	λ free air	$\tau/\lambda^{1/3}$	$w^{1/3}$	$R_1 = \lambda w^{1/3}$ (ft)
1	58.75×10^5	38.0	3.8	15.5×10^5	587×10^5
3	23,250	17.3	2.66	8,740	151×10^3
5	1,740	12.5	2.30	757	9,070
7	317	10.2	2.06	154	1,570
10	50.5	8.4	1.78	28.4	238
15	6.2	6.9	1.55	4.00	27.6
20	1.37	6.0	1.36	1.00	6.02
30	0.157	5.0	1.15	0.137	0.683

SECRET
NAVOED Report 3632

TABLE IV

Radius of Total Evaporation, R_1 , and other
Quantities for Fog

$P_s(\text{psi})$	T (msec)	λ (Free Air)	$T/W^{1/3}$	$W^{1/3}$	$R_1 = \lambda W^{1/3}$ (ft)
0.29	1.14×10^4	~ 100	~ 7.5	1,520	152,000
1.0	3.3×10^3	38	3.8	867	33,000
3	1.1×10^3	17.3	2.66	414	7,150
5	660	12.5	2.3	287	3,590
7	635	10.2	2.06	308	3,142
9	380	8.9	1.88	202	1,798
15	12.4	6.9	1.55	8	55.2
20	2.75	6.0	1.36	2.02	12.12
30	0.32	5.0	1.15	0.278	1.39



SECRET
NAVORD Report 3632

$$F(R) = 4.06 \times 10^5 \frac{W^{11/9}}{R^{2/3}} - 69 cR^3$$

is unchanged. Similarly unchanged is the relation of attenuated pressure viz:

$$P_r = P Z^{.63}$$

P is the pressure obtained at a given distance R when charge W is detonated in clear air; P_r is the pressure obtained at the same distance when W is fired in fog or rain of concentration G; Z is a factor less than unity such that Z W fired in clear air produces pressure P_r at the same value of R.

$$Z = \left[1 - 1.70 \times 10^{-4} \frac{cR^{11/3}}{W^{11/9}} \right]^{9/11}.$$

Pressure attenuation is increased, however, since $R < R_1$ can be larger due to the increase in R_1 .

31. The increase in the pressure attenuation is shown in Tables V, VI, and VII. Comparing the values of P_r from these tables with those in Tables VI, VII, and VIII of reference (3), it is seen that the values of P_r for greater distances than in reference (3) are now valid.

32. There is one more point to be considered regarding the energy available for evaporation of the droplets. The droplets which resulted when the drop was broken up in the fast air stream behind the shock actually did not begin to appear earlier than about 3 milliseconds after the shock front had passed. For small charges this is an appreciable part of the positive phase. Hence, the droplets, after they are produced, do not have the entire positive phase in which to evaporate. This would have the effect that less energy would be used in evaporating the droplets, consequently the attenuation would be less than predicted here. Since no exact data are available from this study regarding the time for the droplets to form after the shock passes, no analytical statement can be made about the attenuation produced. In all probability separate measurements of the time for break-up of liquid drops for each of a series of pressures would have to be made in order to state generally what fraction of the positive phase is available for evaporating the droplets after they have been produced, and this might be considered as a further study to be made as a check on the theoretical work of reference (3).

SECRET
NAVORD Report 3632

TABLE V
Calculation of P_r for 1 lb of Pentolite

		1 lb Pentolite $W = 1.2$	1.2 lb TNT $W^{11/9} = 1.25$				
		$Z = [1 - 1.36 \times 10^{-4} R^{11/3}]^{9/11}$					
P	R	$R^{11/3}$	Z	P_r	$(ZW)^{1/3}$	R_1 (Rain or Fog)	
C = 5							
10	8.9	3,000	Imaginary				
20	6.4	900	0.465	12.3	0.824	5.01	P_r not valid
25	5.5	532	0.692	19.8	0.940	5.81	P_r valid
30	5.35	470	0.73	24.6	0.956	5.92	P_r valid
33	5.1	395	0.775	28.0	0.977	6.02	P_r valid
40	4.7	295	0.834	35.6			P_r valid
C = 10							
33	5.1	395	0.515	21.6	0.849	5.19	Valid
37	4.9	340	0.604	26.9	0.898	5.52	Valid
40	4.7	295	0.66	30.8	0.925		Valid
C = 20							
40	4.7	295	265	17.3	0.683	4.07	Not Valid
50	4.2	210	205	32.5	0.844	4.74	Valid
C = 40							
60	4.0	162	0.175		0.594	3.49	Not Valid
70	3.77	130	0.367	37.2	0.76	4.58	Valid

SECRET
NAVED Report 3632

TABLE VI

Calculation of P_T for 20 KT Atomic Bomb

Using equivalence of 0.5 $W = 20 \times 10^6$ lbs TNT							
$\therefore R^{11/9} = 8.4 \times 10^8$							
$Z = [1 - 2.02 \times 10^{-13} R^{11/3}]^{9/11}$							
P	R	$R^{11/3}$	Z	P_T	$(ZW)^{1/3}$	R_1 (Rain, Fog)	
C = 1							
8	2560	3.12×10^{12}	0.445	4.8	207	2315	P_T not valid
10	2280	2.06×10^{12}	0.641	7.5	234		P_T Valid
12	2100	1.54×10^{12}	0.738	9.9			P_T Valid
15	1860	0.965×10^{12}	0.838	13.4			P_T Valid
20	1650	0.63×10^{12}	0.895	18.6			P_T Valid
C = 5							
18	1725	7.37×10^{11}	0.528	8.9	187	1940	P_T Valid
20	1690	6.3 "	0.440	11.9			P_T Valid
30	1360	3.06 "	0.739	24.8			P_T Valid
40	1210	2.02 "	0.835	35.8			P_T Valid
C = 0.2							
3	4700	2.9×10^{13}	Imaginary				
5	3370	0.86 "	0.706	4.0	242	2750	Not Valid
8	2560	0.312 "	0.901	7.5	252	2800/2870	Valid
10	2280	0.206 "	0.932	9.56	267	2900/3050	Valid

SECRET
NAVORD Report 3632

TABLE VII

Calculation of P_r for 1 Megaton Atomic Bomb

1 Megaton - using 0.5 equivalence $W = \frac{2000 \times 10^6}{2} = 10^9$ lbs							
$\therefore W^{11/9} = 10^{11}$							
$Z = [1 - 1.70 \times 10^{-15} eR^{11/3}]^{9/11}$							
P	R	$R^{11/3}$	Z	P_r	$(ZW)^{1/3}$	R_1 (Rain, Fog)	
C = 1							
6.5	10500	5.54×10^{14}	0.104	1.56	470	4900 7960	Not Valid
7	10100	4.8 "	0.252	2.94	632	7430 10670	Valid for fog
8	9400	3.7 "	0.444	4.8	763	8740 25600	Valid for fog
9	8850	3 "	0.56	6.22			Valid
10	8400	2.45 "	0.644	7.57	863		Valid
12	7700	1.8 "	0.742	9.94			Valid
15	6900	1.2 "	0.83	13.3			Valid
C = 5							
15.5	6800	1.12×10^{14}	~0.07	2.9	410	4550 6950	Valid for fog
16	6700	1.08 "	0.13	4.4	506	5800 10900	Valid for fog
17	6500	0.95 "	0.26	7.2	638	7500 17500	Valid
18	6350	0.88 "	0.322	8.8	685		Valid
20	6000	0.71 "	0.474	12.2	780		Valid
40	4500	0.25 "	0.824	35.4			Valid
C = 0.2							
3.5	15400	22×10^{14}	0.325	1.72	687	8300 20500	Valid for fog
4	14200	17 "	0.495	2.57	790	10238	Valid for fog
5	12250	9.7 "	0.721	4.06	897	11793	Valid for fog
7	10100	4.8 "	0.864	6.4	953		Valid

SECRET
NAVORD Report 3632

REFERENCES

1. W. G. Penney, Use of Gadget in Rain or Fog, Feb 6, 1944, Secret.
2. W. G. Penney, Loss of Performance of H.E. Bombs and Atomic Bombs when Exploded in Fog or Rain, ARE Report No. 1/48, Sep 1948, Secret.
3. G. K. Hartmann, The Effect of Rain or Fog on Air Blast, NAVORD Report 2944, Aug 1, 1953, Secret.
4. P. Z. Kalavski, A High Speed Recording System Using the Velocity Method to Determine the Peak Pressure Produced in Air by Explosions, NAVORD Report 2167, Feb 25, 1952, Unclassified.
5. W. R. Lane, Shatter of Drops in Streams of Air, Industrial and Engineering Chemistry, Vol. 43, June 1951, pp 1312-1317.
6. Sir Geoffrey Taylor, Min. of Supply Paper AC 10647/phys. c 69(1949).

SECRET
NAVORD Report 3632

DISTRIBUTION LIST

	Copies
Chief of the Bureau of Ordnance (Re2c)	5
Chief of the Bureau of Ordnance (Rem)	1
Chief of Bureau of Medicine and Surgery	2
Chief of Bureau of Ships	2
Chief of Bureau of Yards and Docks	2
Chief of Naval Research	2
Chief of Ordnance, Department of the Army, Washington, DC	2
Commanding General, Air Materiel Command, Wright-Patterson Field, Air Force Base, Dayton, Ohio	2
Commander, Naval Ordnance Test Station, Inyokern, China Lake, California	3
Director, Ballistic Research Laboratories, Aberdeen Proving Ground, Maryland	2
Director, Naval Research Laboratories, Washington, D.C.	2
Chief, Armed Forces Special Weapons Program, Pm 1B684, The Pentagon, Washington, D.C.	10
Applied Physics Laboratory, Johns Hopkins Univ., Silver Spring, Maryland, INM, Silver Spring, Md.	1
Dr. E. F. Cox, Sandia Corporation, Sandia Base, Albuquerque, New Mexico, INM, Los Angeles, Cal	1
Mr. S. Raynor, Assistant Chairman, Armour Research Foundation, Illinois Institute of Technology, Chicago 16, Ill., via INM, Chicago, Ill	1
Dr. E. B. Doll, Stanford Research Institute, Stanford, Calif., via Armed Forces Special Weapons Project, P.O. Box 2610, Washington, D.C.	1
Frank A. Parker, Director, Project Squid, Princeton University, Princeton, New Jersey, via INM, Newark, New Jersey	1
Director, Bureau of Mines, Washington, D.C. ATTN: Stephen L. Windes, Eastern Experiment Station	2
Chief of Engineers, Temp. Bldg. T-7, Room G-425, Gravelly Point, Virginia	1
Chief Signal Officer, Department of the Army, Washington, DC	2
Director, Operations Research Office, 6410 Connecticut Ave., Chevy Chase, Maryland	1
Commanding Officer, U. S. Naval Radiological Defense Laboratory, San Francisco 24, Cal	1
Director of Operations, Headquarters, USAF, Washington, DC ATTN: Operations Analysis Div	1
Director of Intelligence, Headquarters, USAF, Washington, DC ATTN: Phys. Vul. Branch, Air Targets Division	1
Commanding General, Strategic Air Command, Offutt Air Force Base, Nebraska	1
Commanding General, Air Research and Development Command, P.O. Box 1395, Baltimore, Md	3
Commanding General, Air Materiel Command, Wright- Patterson Air Force Base, Dayton, Ohio, ATTN: Air Installation Division	1

SECRET

SECRET
NAVED Report 3632

DISTRIBUTION LIST

	Copies
Commanding Officer, Air Development Squadron 5, USN Air Station, Moffett Field, Cal	1
Commanding Officer, USN Medical Center, Bethesda, Md	1
Commanding Officer and Director, USN Electronics Laboratory San Diego, Cal. ATTN: Code 210	1
Commanding Officer, USN Radiological Defense Laboratory, San Francisco, Cal ATTN: Technical Information Divn	2
Commander, Naval Air Development Center, Johnsville, Pennsylvania	1
Commanding Officer and Director, David Taylor Model Basin, Washington 7, D.C. ATTN: Library	1
Asst. for Atomic Energy, Headquarters, USAF, Washington, D.C. ATTN: DCS/O	1
Asst. for Development Planning, Headquarters, USAF, Washington, D.C.	1
Director of Operations, Headquarters, USAF, Washington, D.C.	1
Director of Plans, Headquarters, USAF, Washington, D.C. ATTN: War Plans Division	1
Directorate of Research and Development Armament Division, DCS/D, Headquarters, USAF, Washington, D.C.	1
Commanding General, Northeast Air Command, APO 862, c/o Postmaster, New York, N.Y.	1
Directorate of Intelligence, Headquarters, USAF, Washington, D.C.	2
Commanding General, Air Defense Command, Ent AFB, Colorado	2
Commanding General, Lowry AFB, Denver, Colo ATTN: Dept. of Armament Training	2
The RAND Corporation, 1500-4th St., Santa Monica, Cal. ATTN: Nuclear Energy Division, via INM Los Angeles, Cal	2
Asst. for Civil Defense, OSD, Washington, D.C.	1
Executive Secretary, Committee on Atomic Energy, Research and Development Board, Rm 3E1075, Pentagon, Washington, DC.	2
Executive Secretary, Military Liaison Committee, PO Box 1814, Washington, D.C.	1
Commandant, National War College, Washington, D.C. ATTN: Classified Records Section, Library.	1
Commandant, Armed Forces Staff College, Norfolk, Va. ATTN: Secretary	1
Commanding General, Field Command, AFSWP, P.O. Box 5100, Albuquerque, New Mexico	5
University of California Radiation Laboratory, P.O. Box 808, Livermore, Cal. ATTN: M. Folden, via INM San Francisco	1

SECRET

NAVFORD Report 3632

DISTRIBUTION LIST

	Copies
Commanding General, Special Weapons Center, Kirtland Air Force Base, New Mexico	1
Asst. to Special Assistant, Chief of Staff, U.S. Air Force, Pentagon, Washington, D.C.	1
Commanding General, Wright Air Development Center, Wright-Patterson Air Force Base, Dayton, Ohio	1
Commanding Officer, Air Force Cambridge Research Center, 230 Albany Street, Cambridge, Mass	1
Director, Weapons System Evaluation Group, Office of the Secretary of Defense, Washington, DC	3
Commander, Joint Task Force 132, Washington, D.C.	1
Director, Division of Military Applications, U.S. Atomic Energy Commission, 1901 Constitution Ave., Washington, D.C.	1
Ballistic Research Laboratories, Aberdeen Proving Ground, Md. ATTN: Mr. W. E. Curtis	1
ATTN: Dr. C. W. Lampson	1
Dr. S. J. Fraenkel, Armour Research Foundation Technology Center, Chicago 16, Ill. via INM Chicago, Ill	1
University of Maryland, via INSORD, APL, Silver Spring, Md.	1
George Washington University, via INM, Baltimore, Md.	1
Superintendent of Naval Post Graduate School, Monterey, Cal	1
Department of the Air Force, Rm 5B271, Pentagon, Washington, DC ATTN: Dr. James C. Mouzon	1
Department of the Air Force, Director of Research and Development, Pentagon, Washington 25, D.C. ATTN: Dr. R. C. Grassy	1
Commanding General, Tactical Air Command, Langley AFB, Va. ATTN: Documents Security Branch	1
U. S. Naval Engineering Experiment Station, Annapolis, Md. ATTN: Miss Beate E. Day, Statistician	1
Prof. Werner Goldsmith, Dept. of Engineering Design, University of California, Berkeley, Cal. via INM, San Francisco, Cal	1
The Superintendent, U.S. Military Academy, West Point, N.Y. ATTN: Prof. of Ordnance	2
Chief of Research and Development, D/A, Washington, DC	1
Commanding Officer, Picatinny Arsenal, Dover, N.Y. ATTN: ORDBB-TK	1
Director, Technical Documents Center, Evans Signal Laboratory, Belmar, N.J. via INM New York	1
Director, Waterways Experiment Station, P.O. Box 631, Vicksburg, Miss. ATTN: Library	1
Chief of Naval Operations, D/N, Washington, D.C. ATTN: Op-36	1
Chief of Naval Operations, D/N, Washington, D.C. ATTN: Op-374 (OEG)	1
Chief, Bureau of Ships, D/N, Washington, D.C. ATTN: Code 348	1
Chief, Bureau of Aeronautics, D/N, Washington, D.C.	1
President, U. S. Naval War College, Newport, R.I.	1
Commander, Air Force, U.S. Pacific Fleet, Naval Air Station, San Diego, Cal	1

NAVORD Report 3632

DISTRIBUTION LIST

Copies

Los Alamos Scientific Laboratory, Report Library,
P.O. Box 1663, Los Alamos, New Mexico,
ATTN: Helen Redman, via INM Los Angeles, Cal 1
Sandia Corporation, Classified Documents Division,
Sandia Base, Albuquerque, New Mexico,
ATTN: Wayne K. Cox, via INM Los Angeles, Cal 1
Dr. John Van Neumann, The Institute for Advanced Studies,
Princeton University, Princeton, N.J. via INM, Philadelphia . . . 1
Dr. Walker Blackney, Palmer Physical Laboratory,
Princeton University, Princeton, N.J. via INM, Philadelphia . . . 1
Dr. Walter A. MacNair, Sandia Corporation, Sandia Base,
Albuquerque, N. Mexico, via INM Los Angeles, Cal 1
Prof. Hoyt C. Hottel, Massachusetts Institute of
Technology, Cambridge 39, Mass. via INM Boston 1
Dr. David T. Griggs, Institute of Geophysics, University of
California, Los Angeles, Cal. via INM Los Angeles 1
Dr. Frederick Reines, Los Alamos Scientific Laboratory,
P.O. Box 1663, Los Alamos, New Mexico, via INM
Los Angeles 1

UNCLASSIFIED

UNCLASSIFIED